The removal of Pb(II) ions from aqueous solutions by immobilized (*Chlorophyta*) macroalgae: an equilibrium, kinetic, and desorption-regeneration study

Daad Saad Alobaidi[a], Abeer I. Alwared[b],*

[a]*Ministry of Youth and Sports, Baghdad, Iraq, email: d.dawood1011@coeng.uobaghdad.edu.iq*
[b]*Department of Environmental Engineering, College of Engineering, University of Baghdad, Iraq,*
email: dr.abeer.wared@coeng.uobaghdad.edu.iq

ABSTRACT

This study presents the synthesis of biosorbent by the immobilization of green algae (*Chlorophyta*) into calcium alginate as a supporting composite for the removal of heavy metals. The batch adsorption system was employed to investigate the effectiveness of the algae-alginate synthesized beads (AASB) in lead removal from an aqueous solution. Since pH 5 produced the greatest removal efficiency of Pb(II) ions, it reveals that the pH significantly affects the adsorption of Pb(II) ions using AASB as an adsorbent. Results showed that the ideal working conditions for AASB were: 5 g/L of AASB, 120 min of contact time, pH value of 5, and 200 rpm agitation speed, which achieved roughly 90.98% removal efficiency and a capacity of 9.0492 mg/g. Several analytical methods, such as Fourier-transform infrared spectroscopy (FTIR), scanning electron microscopy (SEM), and energy-dispersive X-ray spectroscopy (EDS), were used to evaluate the adsorbent's performance and investigate its adsorption mechanism. FTIR analysis showed the engagement of hydroxyl, amino, and carboxyl functional groups during Pb(II) ions adsorption, At the same time, the metal cations are adsorbed on the surface of the algal biomass, which is demonstrated by SEM to have an amorphous superficial structure, while EDS spectra showed the presence of elements that are favorable for Pb(II) adsorption. The equilibrium isotherm results were well suited to the Freundlich isothermal model, although the adsorption kinetic data is accurately articulated by the pseudo-first-order model. This suggests that heavy metals can be removed from wastewater using AASB which is considered a feasible and effective biosorbent.

Keywords: Adsorption; *Chlorophyta* Algae; Algae-alginate synthesized beads; Pb(II) ions wastewater; Algae characteristics

1. Introduction

Heavy metal contamination is one of the most pressing environmental challenges in our world today. Because heavy metal ions are highly toxic, patient, and have the propensity to accumulate, their existence in water resources has become a significant component in depreciating ecosystem quality [1]. In compliance with the World Health Organization (WHO), the metals with the most significant concern theorized in polluted surface water, groundwater, and industrial wastewater are copper, lead, cadmium, cobalt, chromium, mercury, zinc, and nickel [2]. Heavy metals cause serious environmental risks since they cannot degrade and are hazardous in nature [3]. Many researchers have focused on Pb(II) ions removal which is thought to be carcinogenic heavy metals that are particularly lethal at low concentrations [4,5], It is widely used in battery manufacturing, gasoline combustion, mining, and the electroplating industries [6,7]. The neurological, digestive, immunological, reproductive, and urogenital systems would suffer substantial harm [8,9] once it builds up in the human body and exceeds 0.01 mg/L the permissible limit for Pb contamination in drinking water which was estimated by WHO [10].

* Corresponding author.

Heavy metal ion removal from wastewater is traditionally accomplished using various methods, including ion exchange, electrochemistry, chemical precipitation, solvent extraction, membrane processes, flotation, and sorptive flotation process [11]. These treatment methods are costly, consume immense energy, and sometimes can result in serious secondary pollution. In contrast to this, biosorption is an economical and sustainable technology that can replace traditional wastewater treatment methods. Among biosorbents, those made from alginate derivatives and seaweed (macroscopic algae) have a strong affinity for various metal ions. Biosorbents are excellent for treating hazardous metals from industrial waste since they are less expensive, readily available, and usually biodegradable than commercial synthetic adsorbents [2,12]. When using algae as a biosorbent, some restrictions exist on separating the biomass from the effluent, leading to unsatisfactory pressure drops. Those issues are linked to the biomass's physical properties, including its low density, small particle size, and weak stiffness [13]. These disadvantages might be solved by employing immobilization technology, as it offers mechanical strength, rigidity, appropriate size, and porous properties. Effective immobilization depends on choosing the suitable carrier material. Alginate-based systems have gotten huge attention as immobilization matrixes due to their ease of use, strong biosorption capacity, and low-cost [14,15]. Over the years, brown macroalgae have produced alginate salts, which have been developed into adsorbents because of their selectivity for pollutants, abundance, renewability, and economic viability [16,17].

In contrast to other functional groups like sulfonic acid and a hydroxyl group, alginate has an excess of carboxylic acid groups, which contributes to its strong affinity toward metal ions [18]. The capability of a variety of marine algal biomass to retain different heavy metal ions from an aqueous solution has been demonstrated in countless studies from the literature such as green marine alga, *Ulva lactuca* [19]; brown marine alga *Sargassum filipendula* [20]; blue-green algae [21,22]; single and mixture of algae [23]; *Spirulina* [24]; free and immobilized alginate-*Spirulina* [25]. This investigation aims to determine the ability of algae-alginate synthesized beads (AASB) to remove Pb(II) ions from an aqueous solution at ambient temperature. Many variables such as pH, metal concentration, contact time, dosage, and particle size, are studied during batch studies to estimate the best AASB parameters. In addition, isotherm and kinetic models are considered.

2. Materials and methods

2.1. Materials

Gathered algal was collected from the Al-Yousfya irrigation canal in Baghdad's surroundings/ Iraq where they are found on the water surface, as represented in Table 1 and their microscopic images are shown in Fig. 1. The significant proportion of the classes of algae samples under analysis are as follows (wt.%): 96% of *Chlorophyta* that are divided into 25% of *Mougeotia robusta* and 71% of *Spirogyra subsalsa* while the remaining 4% is *Bacillariophyta* (*Cocconeis pseudomarginata*). The algae were thoroughly rinsed with tap water and then distilled water to remove salt and impurities. In addition, upon being washed, the biomass algae were air-dried for a couple of days and then oven-dried at 60°C for 24 h. Finally, the dried algae were milled with a grinder and then screened to obtain the desired particle size (<63 μm) and then kept in a dry, room temperature environment for future use.

Table 1
Specification of 1 kg of fresh algae

Status of the living organisms	Percentage of the algae biomass (%)	Algal species	Algal aggregates
Roaming on the water surface	25	*Mougeotia robusta* (De Bary) Wittrock	*Chlorophyta*
	71	*Spirogyra subsalsa* Kuetzing	
Attached on the algae	4	*Cocconeis pseudomarginata* (Gregory)	*Bacillariophyta*
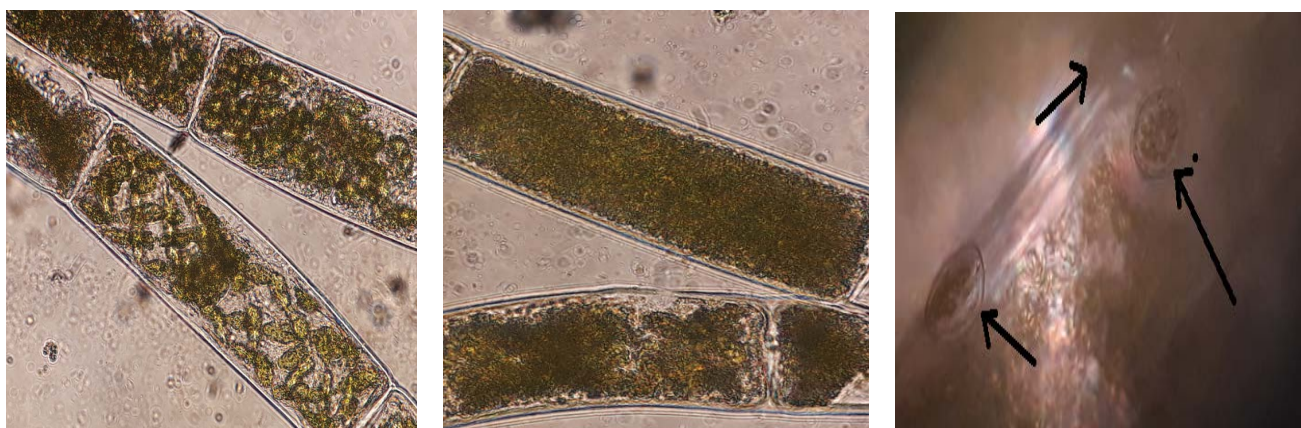
Fig. 1. Microscopic images of the algae sample.

Lead nitrate (Pb(NO$_3$)$_2$, purchased from SIGMA company, USA) was selected as the target pollutant in aqueous solutions. However, for beads, preparation sodium alginate of the chemical structure (NaC$_6$H$_7$O$_6$) and primary source algal polysaccharides derivatives (marine seaweed algae) were manufactured in China and supplied from amazon, and CaCl$_2$ was used. All the chemicals used were of the highest purity available and had an analytical grade.

2.2. Preparation methods

The stock solution of Pb(II) ions was prepared by dissolving the required amount of Pb (NO$_3$)$_2$ in distilled water. Further, dilution was used to get a concentration of (25–100) mg/L, and then the initial pH values of the solution were controlled by adding 0.1 M NaOH or HCl.

Algae-alginate synthesized beads (AASB) were formed by entrapping algae in an alginate matrix caused by ionic polymerization in calcium chloride solution, as follows: the powdered Algal was suspended in an appropriate concentration of sodium alginate solution of 2 w/v% under rapid agitating using a magnetic stirrer to obtain a homogenous solution. An alginate solution containing sodium alginate and 0.5 g powdered algae was gradually added to 100 mL of the solution with continuous stirring to form cohesive gelatin. For AASB formation, prepare a solution of 200 mL

of 0.2 M calcium chloride to harden the composite gel using a 10 mL syringe at 30 cm height as shown in Fig. 2. The AASBs were kept in the solution of calcium chloride for complete hardening for about 24 h or less, and then the beads were rinsed with distilled water many times until neutral pH was achieved. The beads were air-dried for a period of 15 min at room temperature for immediate use.

2.3. Batch adsorption studies

Conical flasks (250 mL in size) were filled with 100 mL of Pb(II) ions solution at the required concentration and biosorbent dosage to conduct batch sorption experiments. Experiments were carried out in the laboratory at room temperature with an initial pH range of 3–6, a biosorbent dosage range of 0.01–2 g/100 mL, an initial Pb(II) ion concentration range of 25–100 mg/L, and a contact time range of 0–180 min. After agitating the flasks for a predetermined amount of time, samples of 10 mL each were collected and analyzed using a flame atomic absorption spectrophotometer (Shimadzu AA680) to measure the concentration of Pb(II) ions.

Using Eqs. (1) and (2), the removal efficiency and the mass of metal ions adsorbed per unit mass of adsorbent, q_e (mg/g), were subsequently calculated, respectively.
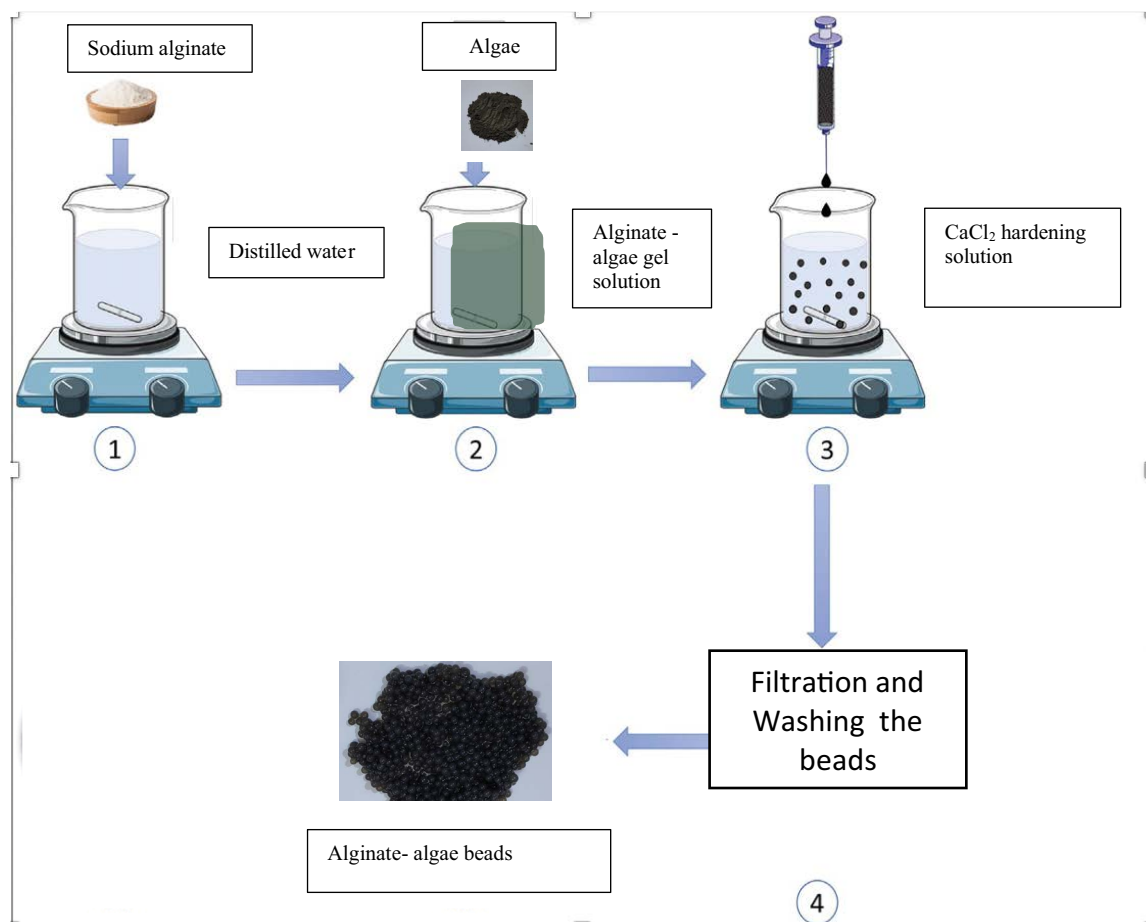
Fig. 2. Preparation procedure of AASB.

$$\text{Removal efficiency}\left(\%\right) = \frac{C_o - C_e}{C_o} \times 100 \tag{1}$$

$$q_e = \left(C_0 - C_e\right) \times \frac{V}{m} \tag{2}$$

where C_o and C_e represent the initial and equilibrium concentrations (mg/L) of metal ions, V represents the volume (L) of the solution sample, and m represents the mass (g) of the adsorbent (g).

Other parameters were kept constant while studies of adsorption isotherms and kinetics were conducted at various concentrations (5–125) mg/L and contact times (0–180) min.

Using Fourier-transform infrared (FTIR) with a range of 400–4,000 cm⁻¹ (Tensor 27, Bruker, Germany) analysis, scanning electron microscopy (SEM), and energy-dispersive X-ray spectroscopy (EDS) (ZEISS model; Sigma VP), the sorption mechanisms were specified through the identification of the active functional group, surface morphology, and changes in shape responsible for Pb(II) ion binding on the AASB.

3. Results and discussion

3.1. Characteristics of AASB

3.1.1. Fourier-transform infrared spectroscopy

Fig. 3 interprets the FTIR analysis of the biosorbent before and after Pb(II) adsorption, which illustrates the functional groups involved in lead adsorption. Numerous *Chlorophyta* algae possess typical algal cell walls composed of an amorphous matrix and a fibril skeleton (primary cellulose). Alginic acid, chitin, and xylan are polysaccharides that comprise the

algal cell wall and are known to serve as metal-binding sites. The algal surface contains groups that can bind metal ions, including carboxyl, hydroxyl, sulfhydryl, phosphate, sulfate, imidazole, and amine. As part of their metal uptake mechanism, metal ions bind to the surface of algae, which is then followed by internalization. Required is one of two algal biosorption mechanisms. (1) ion-exchange method in which Ca, Mg, Na, and K ions on the algal surface displace them; (2) complexing of metal ions and functional groups [3,26]. Table 2 lists the functional group's bonds before and after adsorption with respect to the number of bonds (single, double, and triple). Accordingly, Table 2 shows the peak around 1,630 cm⁻¹ shifts to 1,600.68 cm⁻¹ following biosorption, indicating site-specific interactions. This may be because the free carboxyl group has changed into a carboxylate group, which typically happens during the reaction between Pb(II) ions and the carboxyl group. The strong peak at around 3,329.52 cm⁻¹ shifted to 3,324.22 cm⁻¹ is the result of O–H stretching vibrations. Also, FTIR spectra (Fig. 4) reveal that the peaks at 2,353.61; 2,315.59; 2,126.35; and 1,957 cm⁻¹ demonstrated minor differences after Pb(II) ions treatment that appeared in triple and double bond region. However, there were a few peaks in the fingerprint region that had a small shift (from 1,417.3 to 1,414.87 cm⁻¹, 1,084.54 to 1,082.51 cm⁻¹, 944.31 to 938.86 cm⁻¹, 888.47 to 885.42 cm⁻¹ and 591.98 to 599 cm⁻¹), denoting the involvement of hydroxyl, amino, and carboxyl groups during Pb(II) adsorption. 1,417 cm⁻¹ ascribed to COO⁻, The COO⁻ functional group's presence facilitated the sorption of Pb(II) ions on AASB [27].

3.1.2. Scanning electron microscopy-energy-dispersive X-ray analyzer

Fig. 4 illustrates SEM images of AASB prior to and following adsorption. The SEM micrograph revealed that the
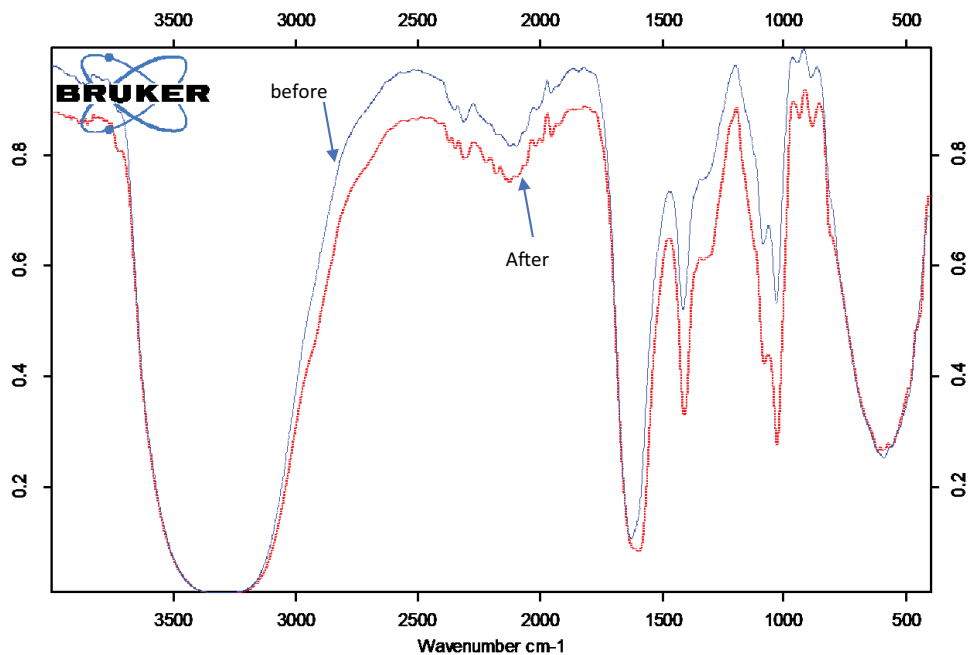
Fig. 3. FTIR of AASB before and after adsorption.

Table 2
FTIR absorption bands of AASB adsorbent before and after adsorption

	Single bond (O–H, N–H, C–H)	Triple bond (C≡C, C≡N)	Double bond (C=C, C=N, C=O)	Fingerprint
Before adsorption	3,329.52	2,353.61 2,315.59 2,126.35	19,571,630.01	1,417.3 1,084.54 1,030.8 944.31 888.47 591.98
After adsorption	3,324.22	2,351.7 2,318.14 2,187.28 2,130.69	1,958.44 1,600.68	1,414.87 1,082.51 1,030.51 938.86 885.42 599

AASB surface had pores and a dense structure. As illustrated by Fig. 4a, in the alginate matrix, the images demonstrate a crosslinked polymer that has developed between the algae. Due to adhesion and effective dispersion in the algae-alginate composite matrix, beads are dense in nature, while Fig. 4b depicts the amorphous surface structure of algal biomass where metal cations are adsorbed, to elucidate AASB components in greater detail, Fig. 5 displays the EDS spectrum. It displays the sodium content, which is derived from alginate. AASB contains carbon, oxygen, and calcium, the main constituents of alginate and algae. EDS spectra describe the metal and element peaks as well as the oxygen from the alginate on the surface of the synthesized beads.

3.2. Optimization of biosorbent bead preparation

Fig. 6 displays the effect of sodium alginate concentration 1, 2, 3, and 4 w/v% in the preparation of the immobilized algae beads on lead ion removal as the powdered algae are kept constant. As seen in this figure, the concentration of sodium alginate has little effect on lead removal percentage. The highest removal efficiency is achieved when sodium alginate is 2 w/v, and the biosorbent preparation and moulding of the beads are easily and suitably done. On the other hand, a 3% and 4% concentration of sodium alginate is excessively high for the favorable preparation of adsorbent beads. This is because the matrix becomes denser and has smaller pores as the concentration of alginate gel rises, which restricts the uptake of nutrients or other macromolecules [28]. Thus, the optimal volume percentage of sodium alginate in the preparation of biosorbent beads is 2%.

3.3. Affecting parameters

3.3.1. Initial pH value

Other factors to consider, in addition to the adsorbent's surface charge, are the adsorbate's speciation and degree of ionization, which are all known to be affected by pH values, which is regarded as an essential parameter in the adsorption process [29]. As demonstrated in Fig. 7, the pH effect on Pb(II) adsorption by AASB was investigated at various pH values ranging from 3 to 6. The removal efficiency was 88.26%, making pH 5 the optimal pH value in this study, a little bit higher than other pH values. The removal percentage increased with the increase of pH value until equilibrium is reached. In this experiment, the pH value does not exceed 6 because of lead precipitation as lead hydroxide. With respect to Higher pH values that resulted in deprotonation, which generated a more negatively charged adsorbent surface and promoted better absorption of Pb(II) ions by electrostatic attraction [30]. Abdulkareem and Alwared [31], state that the removal efficiency was reduced as a result of competition between lead ions and solution protonation, which reduces lead ions passage at lower pH values. Hence functional groups carrying negative charges and becoming exposed as a result of deprotonation, such as carboxyl, phosphate, imidazole, and amino groups, the removal efficiency begins to increase.

3.3.2. Adsorbent dosage

At various AASB dosages 0.1–20 g/L, the adsorbent dosage effect on the adsorption of Pb(II) ion was studied, and the results are plotted in Fig. 8. According to this figure, the amount of adsorbent utilized during adsorption has a notable impact on the removal efficiency. The removal efficiency of Pb(II) ions increased with adsorbent dosage due to the adsorbent's increasing surface area and the availability of additional adsorption sites. At the lowest adsorbent dosage 0.1 g, the removal efficiency of Pb(II) ions was 14.04%. Since there are fewer adsorbent sites, metal ions must compete for the few available spaces, resulting in a slower rate of adsorption [32].

When the maximum adsorbent dosage of 20 g/L and dosage of 5 g/L of AASB were used, the achieved removal efficiencies were 97.83% and 90.98%, respectively. Adsorption sites for Pb(II) ions increased at higher adsorbent dosages and stayed unsaturated throughout the adsorption process. Although, further increase in AASB dosage past this point >7.5 g showed no discernible increase
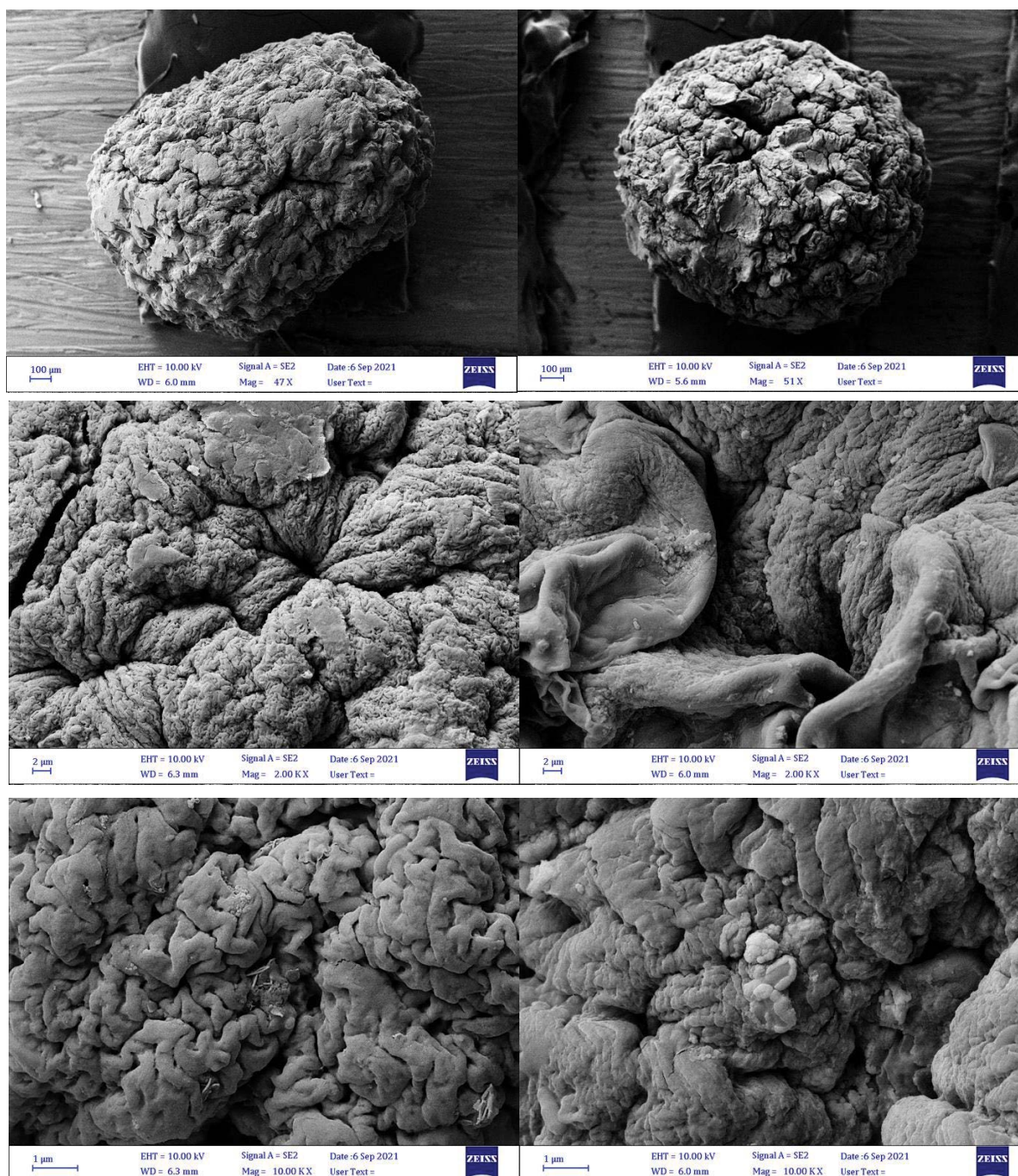
Fig. 4. SEM micrograph of AASB.

in Pb(II) adsorption capacity and removal at which equilibrium is reached. This is ascribed to the saturation of the adsorbent site, which prevents the uptake of additional metal ions [33]. After the dosage exceeded 7.5 g/L, Due to minimal Pb(II) ion concentration, specific active adsorption sites on the adsorbent were still unsaturated. The increased functional groups interacted with Pb(II) ions in the solution to saturate the adsorption sites, thereby facilitating Pb(II) ion adsorption. Regarding economic aspects and treatment efficacy, the optimal dosage of AASB for further

experiments was 5 g/L. Mahmood et al. demonstrated that the increase in alginate-calcium carbonate beads over the range of 0.2–1.5 g/100 mL exhibited a remarkably favorable impact on cadmium ion removal [34]. These results were in agreement with the finding of [35].

3.3.3. Metal concentration and contact time

The initial concentration of metal ions considerably impacts how well an alginate-based adsorbent removes
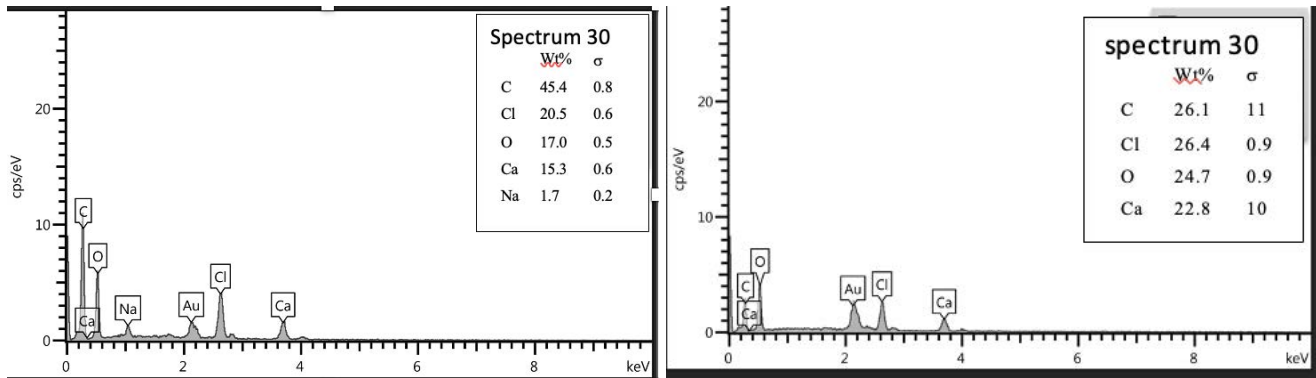
Fig. 5. EDS spectra of AASB.
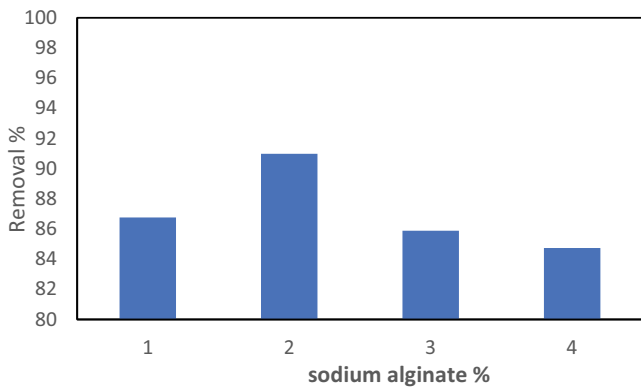
Fig. 6. Sodium alginate w/v effect on the percentage of Pb(II) removal.
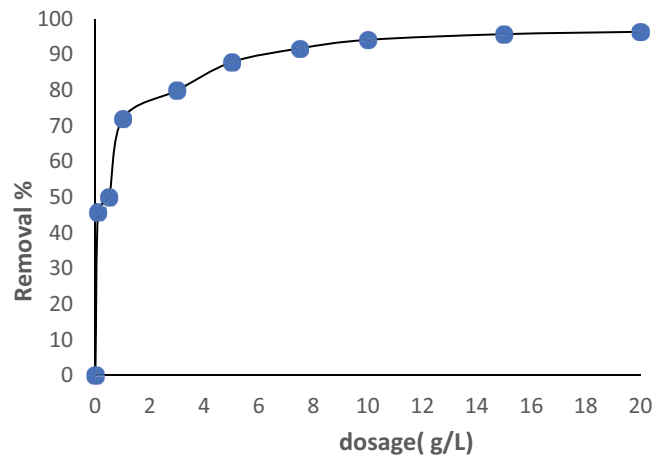
Fig. 8. Adsorbent dosage effect on the percentage of Pb(II) removal by AASB.
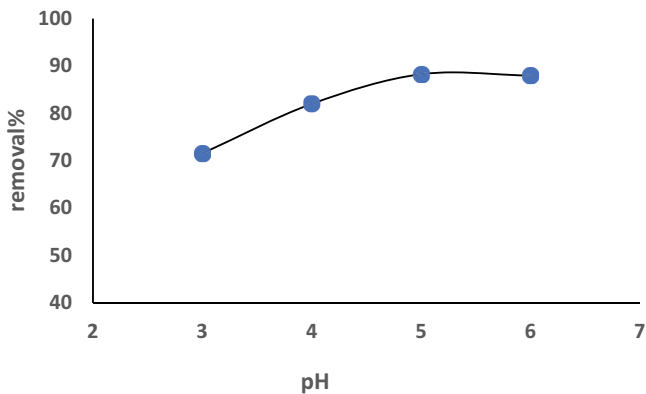
Fig. 7. pH effect on the percentage of Pb(II) ions removal by AASB.
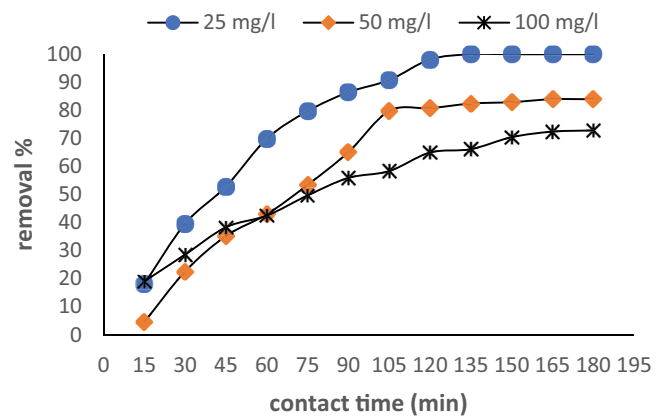
Fig. 9. Initial concentration effect on the percentage of Pb(II) removal by AASB.

metal ions. In the present work, the adsorption of Pb(II) ions on AASB was evaluated with various initial concentrations of 25–100 mg/L. Fig. 9 demonstrates the removal efficiency of Pb(II) ions at various concentrations vs. contact times. As observed, the removal of Pb(II) ions exhibits two distinct phases: a rapid phase within the first 100 min and a slower phase that carries on until equilibrium is reached. As shown, in most cases, 120 min was enough to maintain saturation

in Pb(II) ions adsorption capacity by AASB for all metals concentrations.

Mainly, when the amount of adsorbent is constant, the removal efficiency typically declines as Pb(II) ion concentration increases. This results from high metal ion concentrations that saturate the adsorption sites on the adsorbent

surface completely. Because there were more accessible adsorption sites on adsorbents than initially metal ions, the removal efficiency is high at low metal ion concentrations. Conversely, insufficient adsorption sites would result in low metal adsorption as the metal ion concentration increases [17,36].

As depicted in Fig. 10, a significant increase in the adsorption capacity of AASB with varying initial concentrations may influence the sorption kinetics of the ion. As the Pb(II) ion concentration increases from 25 to 100 mg/L, the adsorption capacity of AASB for the initial 120 min increases from 4.9 to 12.41 mg/g. As the initial concentration of Pb(II) on the beads increases, the beads' ability to absorb Pb(II) becomes constrained, resulting in slower diffusion. At low initial Pb(II) concentrations, the limited number of accessible adsorption sites facilitates mass transfer between the aqueous and adsorbent phases. However, with a high initial concentration, there are more adsorption sites, which increases the probability that Pb(II) ions will bind to the adsorbent surface [37]. The results indicate that the initial Pb(II) concentration was a crucial element in determining the contact time required to achieve maximal Pb(II) ion uptake by the AASB biosorbent.

3.3.4. Particle size

Fig. 11 displays the effect of the particle size of the AASB, which ranges from 1 to 8 mm, on the removal efficiency of Pb(II) ions. Due to the increase in adsorbent surface area, the removal efficiency decreased as the size of the beads increased. This is consistent with the conclusion of [38], which states that a greater surface area corresponds to a greater adsorption capacity and a smaller surface area corresponds to lower adsorption.

3.3.5. Agitation speed

Employing 50 mg/l of Pb(II) ion in 100 mL solution in order to maximize the agitation speed for higher Pb(II) ion adsorption. At 5 pH value, 0.5 g AASB were added to the solution, and the adsorption time was 120 min. Various agitation speeds 100, 200, and 300 rpm were performed. As displayed in Fig. 12, at higher agitation speeds, fewer Pb(II) ions were adsorbed by AASB compared to those at lower agitation speeds. Meanwhile, after a certain point, adsorption efficiency was reduced when the agitation speed was increased. The weakly bound metal ions that tend to collide with the adsorbent particles with high kinetic energy may detach at high speed, decreasing adsorption efficiency [39,40]. The agitation speed of 200 rpm showed the best adsorption efficiency.

3.4. Desorption and reusability

Subsequent adsorption–desorption–regeneration cycles were utilized to study the AASB's reusability. Prior to the desorption experiment, the Pb(II)-ion-packed AASB was placed in a flask of 100 mL of desorbing agent (distilled water). The mixture was agitated for 120 min at 200 rpm. Eq. (3), the desorption efficiency of lead ions on AASB was computed by dividing the number of lead ions adsorbed by the number of lead ions desorbed.

$$\text{Desorption efficiency}\% = \frac{\text{number of metal ions desorbed}}{\text{number of metal ions adsorbed}} \times 100 \tag{3}$$
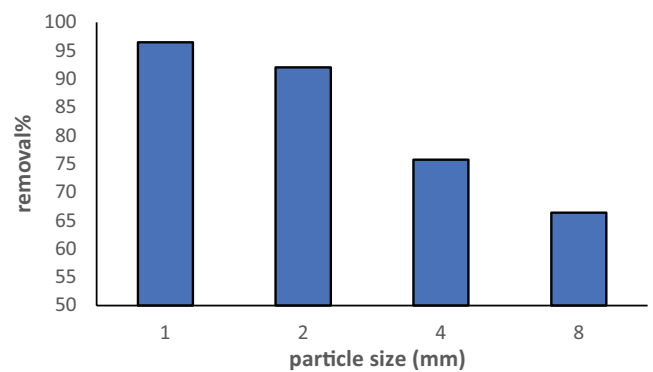
Fig. 11. Particle size effect on the percentage of Pb(II) removal by AASB.

Fig. 10. Initial concentration effect on the biosorption capacity of Pb(II) by AASB.
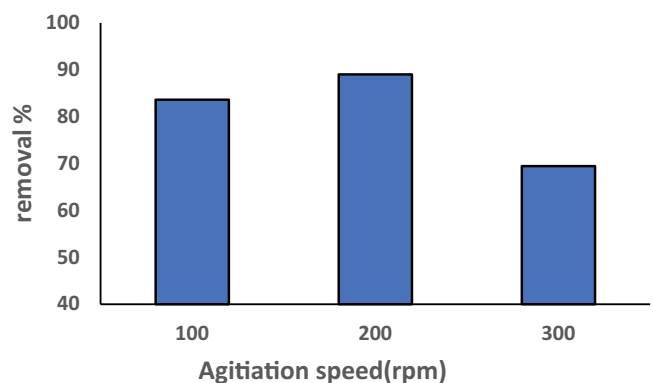
Fig. 12. Agitation speed effect on the percentage of Pb(II) removal by AASB.

Fig. 13 shows the desorption efficiencies for lead ions using distilled water as a desorbing agent. At the end of the experiment within 90 min, 37.8325%, 38.47%, and 38.96% of Pb(II) ions were recovered from the AASB adsorbent for desorption 1, 2, and 3, respectively. A minimal increase in desorption efficiencies was noticed (roughly 1%) in the second desorption cycle (desorption 2) and third cycle (desorption 3) probably as a result of lead build-up that was unable to release during later adsorption.

Desorption depends on contact time. Therefore, the residence time is highly important since it determines how long the desorbing agent will be in contact with the metal-packed adsorbent [41]. However, residence time must also be relatively short to prevent the degradation of the biomass and lengthen its lifetime for recycling [42]. In this work, the desorption time was 90 min, while at time 120 min the desorption efficiency decreased.

In the reusability experiment, Pb(II) ions-loaded AASB was thoroughly rinsed three times with distilled water and then mixed again in a flask of 100 mL of wastewater containing 50 mg/l lead concentration and repeated four times. Fig. 14 demonstrates the effect of reusing the AASB three times as it shows the removal percentage decreased from 90.98% to 56.44% in the fourth trial due to beads saturation with Pb(II) ions. The 2nd adsorption gives 88.2% removal which indicates the AASB can be reused up to three times before it loses its efficiency.
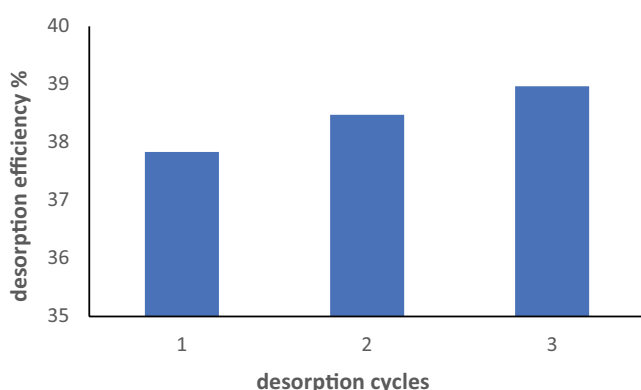
Fig. 13. Desorption effect on the recovery of Pb(II) from lead-loaded AASB.
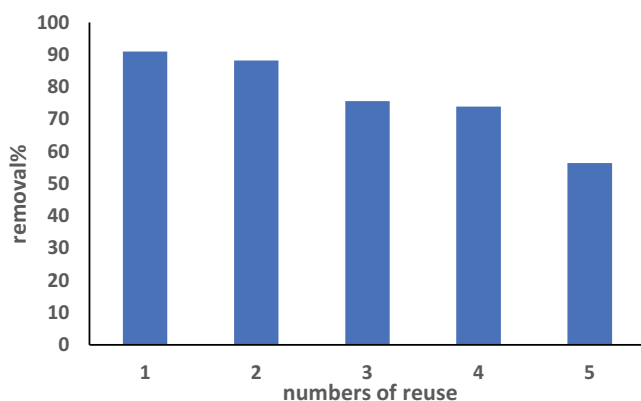
Fig. 14. Reusability of Pb(II) loaded-AASB.

3.5. Adsorption isotherm

The adsorption isotherm describes the relationship between the amount of bio-sorbate adsorbed by the mass of biosorbent at constant temperature and the equilibrium concentration of biosorbate [22]. The sorption isotherm can be used to explain how adsorbate ions are distributed on the adsorbent surface at equilibrium between the liquid and solid phases [43]. The Langmuir isotherm is determined by the monolayer sorption of metal ions on the homogeneous surface of the adsorbent [44]. And the equation can be written as follows:

$$q_e = \frac{q_{max}(K_L)C_e}{1 + K_L C_e} \tag{4}$$

where q_e represents the equilibrium metal adsorbed per gram of adsorbent (mg/g), C_e represents the equilibrium adsorbate concentration (mg/L), q_{max} gives the maximum monolayer capacity (mg/g), and K_L is the Langmuir isotherm constant (L/mg). q_{max} and K_L were calculated using the slope and intercept of the Langmuir plot of $1/q_e$ vs. $1/C_e$, respectively. The Freundlich isotherm illustrates the sorption properties of heterogeneous surfaces, and an empirical equation explains the multilayer adsorption on a heterogeneous surface [45], which can be expressed as follows:

$$q_e = K_f(C_e)^{1/n} \tag{5}$$

where K_f denotes the Freundlich isotherm constant (mg/g), n the adsorption intensity, C_e the equilibrium concentration of the adsorbate (mg/L), and q_e the amount of metal adsorbed per gram of adsorbent at equilibrium (mg/g).

The Langmuir and Freundlich constants for Pb(II) ion adsorption by AASB are presented in Table 3. According to the results, the adsorption of Pb(II) ions by AASB is compatible with the two models. However, the Freundlich model had a marginally higher R^2 coefficient value ($R^2 = 0.995$) than the Langmuir model ($R^2 = 0.9842$). Moreover, the Freundlich isotherm is a better fit for the experimental results of Pb(II) ions adsorption on AASB, as shown in Fig. 15. The fact that n (2.7778) was greater than 1 indicates that the conditions for adsorption are favorable [46]. Furthermore, the adsorbent has a heterogeneous surface structure with an exponential distribution of active sites, as indicated by the fractional value of $1/n$ of 0.36 ($0 < 1/n < 1$) [47].

3.6. Adsorption kinetics

Adsorption kinetic investigations are preferable because they reveal details regarding the action of adsorbate ions on the adsorbent surface [18]. The biosorption kinetics helps understand the metal ions removal process utilizing the biosorbent regarding the rate constant. Since the biosorption rate affects the solid–liquid interface, the residence time of the sorbate is a crucial variable [48]. In addition, the kinetics parameters offer notable data on the diffusion control, mass transfer, and chemical reaction controls of biosorption processes, all of which are important for planning and modeling the biosorption process [49].

Table 3
Fitted isotherm parameters for Pb(II) adsorption

Models	Parameters			$q_{e,theo.}$	$q_{e,exp.}$
Langmuir	R^2	K_L	q_{max}	0.7423	
	0.9842	0.00235	25.84		7.486
Freundlich	R^2	K_f	n	9.00269	
	0.995	3.38922	2.7778		
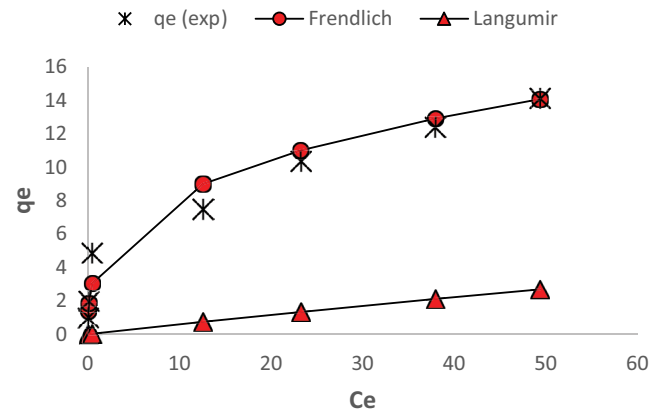
Fig. 15. Langmuir and Freundlich's isotherm calculated and experimental results.

The experimental data from this study were analyzed using pseudo-first-order and pseudo-second-order equations to evaluate the adsorption kinetic studies. Pseudo-first-order demonstrated that the rate of change of solute uptake with time is proportional to the difference between saturation concentration and the amount of solid adsorbed with time [50]. The linear equation of pseudo-first-order is represented as follows:

$$\log(q_e - q_t) = \log q_e - \frac{K_1}{2.303}t \qquad (6)$$

where k_1 is the adsorption constant (min^{-1}) and q_e and q_t represent the amount of metal adsorbed on the adsorbent at equilibrium and time (t), respectively, in mg/g. The value of k_1 was determined by plotting a graph between $\log(q_e - q_t)$ and t. The pseudo-second-order model is based on the idea that the rate-limiting phases are influenced by chemical attraction forces and are close to the entire adsorption process (Siti et al., 2015). The mathematical equation for pseudo-second-order is as follows:

$$\frac{t}{q_t} = \frac{1}{k_2 q_e^2} + \frac{t}{q_e} \qquad (7)$$

where q_e and q_t represent the adsorption capacity in mg/g at equilibrium and at time t (min), respectively, and k_2 represents the model's constant rate (g/mg·min). The pseudo-second-order rate constants were estimated by plotting a graph of t/q_t vs. time (k_2 and q_e). Table 4 lists the kinetic parameters for the adsorption of Pb(II) ions.

Table 4
Kinetic parameters for Pb(II) ion adsorption on AASB

Kinetic model	Fitting parameters	
	R^2	0.9689
Pseudo-first-order	k_1	0.00010222
	q_e	11.9807357
	R^2	0.9491
Pseudo-second-order	k_2	0.02863043
	q_e	19.0114068

As shown in Table 4, the results were more congruent with the pseudo-first-order model with a higher R^2 value ($R^2 = 0.9689$) for the adsorption of Pb(II) ions onto AASB, indicating an approximation between the calculated and experimental q_e values, which indicates that physisorption (pseudo-first-order) rather than chemisorption (pseudo-second-order) is followed in this study. According to several earlier studies, the pseudo-first-order model describes Pb(II) ions' adsorption on alginate composite bead adsorbents [51]. Furthermore, according to Mousa et al. [52], the pseudo-first-order model with a higher R^2 value fit the experimental data of Pb(II) ions removal by calcium alginate and calcium alginate-chitosan adsorbents better than the pseudo-second-order model.

4. Conclusions

The ability of algae-alginate synthesized beads to remove lead(II) ions from the solution was studied using batch adsorption tests. At a pH value of 5 and an initial concentration of 50 mg/L, the adsorption capacity of AASB for Pb(II) reaches its maximum of 7.486 mg/g. According to the results obtained from both isotherm and kinetic experiments, the adsorption of Pb(II) ions is observed to occur rapidly during the first 100 min, reaching equilibrium after approximately 120 min. If we compare the Freundlich isotherm model to the Langmuir isotherm model, we find that the Freundlich model provides a better fit for the adsorption equilibrium data. Compared to the correlation of kinetic data for the adsorption of Pb(II) ions onto AASB, the pseudo-first-order model provided a good fit.

Consequently, the adsorption capacity of the AASB did not significantly decrease after the three-cycle trial. Therefore, the beads were able to be reused in an effective manner. The results of the FTIR analysis and the SEM-EDS images demonstrate that the AASB would be an excellent fit for the role of a lead ion biosorbent because of its considerable adsorption capabilities and exceptional structural stability. According to the findings of this study, the adsorbents can be obtained for a low cost and in large quantities from various sources, and the cost of removal is found to be reasonable. Therefore, the AASB has the potential to be utilized in the treatment of wastewater that contains Pb(II) ions.

Funding

The authors declare that no funds, grants, or other support were received during the preparation of this manuscript.

Competing interests

Authors declare they have no financial interests.

Conflict of interest

- This manuscript has not been submitted to, nor is under review at, another journal or other publishing venue.
- The authors have no affiliation with any organization with a direct or indirect financial interest in the subject matter discussed in the manuscript.
- On behalf of all authors, the corresponding author states that there is no conflict of interest.

Authors contribution

All authors have participated in (a) conception and design, or analysis and interpretation of the data; (b) drafting the article or revising it critically for important intellectual content, and (c) approval of the final version.

Data availability statements

The datasets generated during and/or analyzed during the current study are available from the corresponding author on reasonable request.

Declarations

Ethics approval and consent to participate

Not applicable.

Consent for publication

Not applicable.

Competing interests

The authors declare no competing interests.

References

[1] A.R. Lucaci, D. Bulgariu, M.-C. Popescu, L. Bulgariu, Adsorption of Cu(II) ions on adsorbent materials obtained from marine red algae *Callithamnion corymbosum* sp., Water, 12 (2020) 372, doi: 10.3390/w12020372.

[2] M. Tavana, H. Pahlavanzadeh, M.J. Zarei, The novel usage of dead biomass of green algae of *Schizomeris leibleinii* for biosorption of copper(II) from aqueous solutions: equilibrium, kinetics and thermodynamics, J. Environ. Chem. Eng., 8 (2020) 104272, doi: 10.1016/j.jece.2020.104272.

[3] A. Kwarciak-Kozłowska, L. Sławik-Dembiczak, Biosorption of lead from municipal wastewater by alginate beads, free and alginate-immobilized *Chlorella vulgaris*, Desal. Water Treat., 218 (2021) 303–308.

[4] A. Soenmezay, M.S. Öncel, N. Bektaş, Adsorption of lead and cadmium ions from aqueous solutions using manganoxide

minerals, Trans. Nonferrous Met. Soc. China, 22 (2012) 3131–3139.

[5] N. Yin, K. Wang, L. Wang, Z. Li, Amino-functionalized MOFs combining ceramic membrane ultrafiltration for Pb(II) removal, Chem. Eng. J., 306 (2016) 619–628.

[6] K.H. Kim, A.A. Keller, J.K. Yang, Removal of heavy metals from aqueous solution using a novel composite of recycled materials, Colloids Surf., A, 425 (2013) 6–14.

[7] I. Ali, C. Peng, D. Lin, D.P. Saroj, I. Naz, Z.M. Khan, M. Sultan, M. Ali, Encapsulated green magnetic nanoparticles for the removal of toxic Pb^{2+} and Cd^{2+} from water: development, characterization and application, J. Environ. Manage., 234 (2019) 273–289.

[8] A. Masoumi, K. Hemmati, M. Ghaemy, Low-cost nanoparticles sorbent from modified rice husk and a copolymer for efficient removal of Pb(II) and crystal violet from water, Chemosphere, 146 (2016) 253–262.

[9] M.S. Samuel, S.S. Shah, J. Bhattacharya, K. Subramaniam, N.P. Singh, Adsorption of Pb(II) from aqueous solution using a magnetic chitosan/graphene oxide composite and its toxicity studies, Int. J. Biol. Macromol., 115 (2018) 1142–1150.

[10] R. Ahmad, A. Mirza, Facile one-pot green synthesis of chitosan-iron oxide ($CS-Fe_2O_3$) nanocomposite: removal of Pb(II) and Cd(II) from synthetic and industrial wastewater, J. Cleaner Prod., 186 (2018) 342–352.

[11] A.M. Ridha, Removal of lead(II) from aqueous solution using chitosan impregnated granular activated carbon, J. Eng., 23 (2017) 46–60.

[12] J.F. Fiset, J.F. Blais, P. Riveros, Review on the removal of metal ions from effluents using seaweeds, alginate derivatives and other sorbents, Revue des sciences de l'eau/J. Water Sci., 21 (2008) 283–308.

[13] M. Iqbal, R.G.J. Edyvean, Biosorption of lead, copper and zinc ions on loofa sponge immobilized biomass of *Phanerochaete chrysosporium*, Miner. Eng., 17 (2004) 217–223.

[14] A. Petrovič, M. Simonič, Removal of heavy metal ions from drinking water by alginate-immobilised *Chlorella sorokiniana*, Int. J. Environ. Sci. Technol., 13 (2016) 1761–1780.

[15] L.G. De Araujo, T.R. De Borba, R.V. De Pádua Ferreira, R.L.S. Canevesi, E.A. Da Silva, J.C. Dellamano, J.T. Marumo, Use of calcium alginate beads and *Saccharomyces cerevisiae* for biosorption of ^{241}Am, J. Environ. Radioact., 223 (2020) 106399, doi: 10.1016/j.jenvrad.2020.106399.

[16] M. Kuczajowska-Zadrożna, U. Filipkowska, T. Jóźwiak, Adsorption of Cu(II) and Cd(II) from aqueous solutions by chitosan immobilized in alginate beads, J. Environ. Chem. Eng., 8 (2020) 103878, doi: 10.1016/j.jece.2020.103878.

[17] Z.A. Sutirman, M.M. Sanagi, W.I.W. Aini, Alginate-based adsorbents for removal of metal ions and radionuclides from aqueous solutions: a review, Int. J. Biol. Macromol., 174 (2021) 216–228.

[18] S.N.A. Abas, M.H.S. Ismail, S.I. Siajam, M.L. Kamal, Development of novel adsorbent-mangrove-alginate composite bead (MACB) for removal of Pb(II) from aqueous solution, J. Taiwan Inst. Chem. Eng., 50 (2015) 182–189.

[19] M.M. Areco, S. Hanela, J. Duran, M. Dos Santos Afonso, Biosorption of Cu(II), Zn(II), Cd(II) and Pb(II) by dead biomasses of green alga *Ulva lactuca* and the development of a sustainable matrix for adsorption implementation, J. Hazard. Mater., 213 (2012) 123–132.

[20] A. Verma, S. Kumar, S. Kumar, Biosorption of lead ions from the aqueous solution by *Sargassum filipendula*: equilibrium and kinetic studies, J. Environ. Chem. Eng., 4 (2016) 4587–4599.

[21] Y.A.R. Lebron, V.R. Moreira, L.V.S. Santos, R.S. Jacob, Remediation of methylene blue from aqueous solution by *Chlorella pyrenoidosa* and *Spirulina maxima* biosorption: equilibrium, kinetics, thermodynamics and optimization studies, J. Environ. Chem. Eng., 6 (2018) 6680–6690.

[22] S. Rangabhashiyam, P. Balasubramanian, Characteristics, performances, equilibrium and kinetic modeling aspects of heavy metal removal using algae, Bioresour. Technol. Rep., 5 (2019) 261–279.

[23] H. Abdelkareem, A. Alwared, T.J. Al-Musawi, F. Brouers, A comparative study for the identification of superior biomass facilitating biosorption of copper and lead ions: a single alga or a mixture of algae, Int. J. Environ. Res., 13 (2019) 533–546.

[24] I. Zinicovscaia, A. Safonov, D. Zelenina, Y. Ershova, K. Boldyrev, Evaluation of biosorption and bioaccumulation capacity of cyanobacteria *Arthrospira* (*Spirulina*) *Platensis* for radionuclides, Algal Res., 51 (2020) 102075, doi: 10.1016/j.algal.2020.102075.

[25] M. Villen-Guzman, C. Jiménez, J.M. Rodriguez-Maroto, Batch and fixed-bed biosorption of Pb(II) using free and alginate-immobilized *Spirulina*, Processes, 9 (2021) 466, doi: 10.3390/pr9030466.

[26] A. Ahmad, A.H. Bhat, A. Buang, Biosorption of transition metals by freely suspended and Ca-alginate immobilised with *Chlorella vulgaris*: kinetic and equilibrium modeling, J. Cleaner Prod., 171 (2018) 1361–1375.

[27] J. Feng, J. Zhang, W. Song, J. Liu, Z. Hu, B. Bao, An environmental-friendly magnetic bio-adsorbent for high-efficiency Pb(II) removal: preparation, characterization and its adsorption performance, Ecotoxicol. Environ. Saf., 203 (2020) 111002, doi: 10.1016/j.ecoenv.2020.111002.

[28] S. Banerjee, P.B. Tiwade, K. Sambhav, C. Banerjee, S.K. Bhaumik, Effect of alginate concentration in wastewater nutrient removal using alginate-immobilized microalgae beads: uptake kinetics and adsorption studies, Biochem. Eng. J., 149 (2019) 107241, doi: 10.1016/j.bej.2019.107241.

[29] J. Zhang, J. Shao, Q. Jin, X. Zhang, H. Yang, Y. Chen, S. Zhang, H. Chen, Effect of deashing on activation process and lead adsorption capacities of sludge-based biochar, Sci. Total Environ., 716 (2020) 137016, doi: 10.1016/j.scitotenv.2020.137016.

[30] V. Nejadshafiee, M.R. Islami, Adsorption capacity of heavy metal ions using sultone-modified magnetic activated carbon as a bio-adsorbent, Mater. Sci. Eng., C, 101 (2019) 42–52.

[31] H.N. Abdulkareem, A.I. Alwared, Immobilization dried mix of algae for copper removal, Iraqi J. Agric. Sci., 50 (2019) 800–808.

[32] K.S. Obayomi, J.O. Bello, J.S. Nnoruka, A.A. Adediran, P.O. Olajide, Development of low-cost bio-adsorbent from agricultural waste composite for Pb(II) and As(III) sorption from aqueous solution, Cogent Eng., 6 (2019) 1687274, doi: 10.1080/23311916.2019.1687274.

[33] N. Atar, A. Olgun, S. Wang, Adsorption of cadmium(II) and zinc(II) on boron enrichment process waste in aqueous solutions: batch and fixed-bed system studies, Chem. Eng. J., 192 (2012) 1–7.

[34] Z. Mahmood, A. Amin, U. Zafar, M.A. Raza, I. Hafeez, A. Akram, Adsorption studies of cadmium ions on alginate–calcium carbonate composite beads, Appl. Water Sci., 7 (2017) 915–921.

[35] H.N. Abdulkareem, A.I. Alwared, Performance of immobilized *Chlorella* algae for removing Pb(II) ions from aqueous solution, Iraqi J. Chem. Pet. Eng., 20 (2019) 1–6.

[36] Y.Y. Wang, W.B. Yao, Q.W. Wang, Z.H. Yang, L.F. Liang, L.Y. Chai, Synthesis of phosphate-embedded calcium alginate beads for Pb(II) and Cd(II) sorption and immobilization in aqueous solutions, Trans. Nonferrous Met. Soc. China, 26 (2016) 2230–2237.

[37] E. Yalçın, K. Çavuşoğlu, K. Kınalıoğlu, Biosorption of Cu^{2+} and Zn^{2+} by raw and autoclaved *Rocella phycopsis*, J. Environ. Sci., 22 (2010) 367–373.

[38] P.N. Ikenyiri, C.P. Ukpaka, Overview on the effect of particle size on the performance of wood-based adsorbent, J. Chem. Eng. Process Technol., 7 (2016) 1–4.

[39] M. Yari, P. Derakhshi, K. Tahvildari, M. Nozari, Preparation and characterization of magnetic iron nanoparticles on alginate/bentonite substrate for the adsorptive removal of Pb^{2+} ions to protect the environment, J. Polym. Environ., 29 (2021) 2185–2199.

[40] A.A. Edathil, P. Pal, F. Banat, Alginate clay hybrid composite adsorbents for the reclamation of industrial lean methyldiethanolamine solutions, Appl. Clay Sci., 156 (2018) 213–223.

[41] D. Wankasi, M. Horsfall Jr., A.I. Spiff, Desorption of Pb^{2+} and Cu^{2+} from *Nipa palm* (*Nypa fruticans Wurmb*) biomass, Afr. J. Biotechnol., 4 (2005) 923–927.

[42] S. Indah, D. Helard, A. Binuwara, Studies on desorption and regeneration of natural pumice for iron removal from aqueous solution, Water Sci. Technol., 2017 (2018) 509–515.

[43] M.K. Sureshkumar, D. Das, M.B. Mallia, P.C. Gupta, Adsorption of uranium from aqueous solution using chitosan-tripolyphosphate (CTPP) beads, J. Hazard. Mater., 184 (2010) 65–72.

[44] K.R. Hall, L.C. Eagleton, A. Acrivos, T. Vermeulen, Pore- and solid-diffusion kinetics in fixed-bed adsorption under constant-pattern conditions, Ind. Eng. Chem., 5 (1966) 212–223.

[45] N. Djebri, M. Boutahala, N.E. Chelali, N. Boukhalfa, L. Zeroual, Enhanced removal of cationic dye by calcium alginate/organobentonite beads: modeling, kinetics, equilibriums, thermodynamic and reusability studies, Int. J. Biol. Macromol., 92 (2016) 1277–1287.

[46] V.S. Munagapati, D.S. Kim, Equilibrium isotherms, kinetics, and thermodynamics studies for Congo red adsorption using calcium alginate beads impregnated with nano-goethite, Ecotoxicol. Environ. Saf., 141 (2017) 226–234.

[47] W.H. Zhou, F. Liu, S. Yi, Y.Z. Chen, X. Geng, C. Zheng, Simultaneous stabilization of Pb and improvement of soil strength using nZVI, Sci. Total Environ., 651 (2019) 877–884.

[48] S. Rangabhashiyam, P. Balasubramanian, Characteristics, performances, equilibrium and kinetic modeling aspects of heavy metal removal using algae, Bioresour. Technol. Rep., 5 (2019) 261–279.

[49] S. Gupta, B.V. Babu, Removal of toxic metal Cr(VI) from aqueous solutions using sawdust as adsorbent: equilibrium, kinetics and regeneration studies, Chem. Eng. J., 150 (2009) 352–365.

[50] A. Khaled, A. El Nemr, A. El-Sikaily, O. Abdelwahab, Treatment of artificial textile dye effluent containing Direct Yellow 12 by orange peel carbon, Desalination, 238 (2009) 210–232.

[51] L.P. Ramteke, P.R. Gogate, Treatment of water containing heavy metals using a novel approach of immobilized modified sludge biomass-based adsorbents, Sep. Purif. Technol., 163 (2016) 215–227.

[52] N.E. Mousa, C.M. Simonescu, R.E. Pătescu, C. Onose, C. Tardei, D.C. Culiță, O. Oprea, D. Patroi, V. Lavric, Pb^{2+} removal from aqueous synthetic solutions by calcium alginate and chitosan-coated calcium alginate, React. Funct. Polym., 109 (2016) 137–150.